

## Intensities of two-photon absorptions to low-lying even-parity states in linear-chain conjugated polymers

F. Guo and D. Guo

*Department of Physics, University of Arizona, Tucson, Arizona 85721*

S. Mazumdar

*Department of Physics and The Optical Sciences Center, University of Arizona, Tucson, Arizona 85721*

(Received 10 May 1993)

Interest in the lowest even-parity two-photon states in linear-chain  $\pi$ -conjugated polymers has been largely limited to their energies relative to the lowest odd-parity one-photon state. We show that the intensities of the two-photon absorptions to even-parity states that occur below the lowest one-photon states should be tiny in the infinite chain, because of cancellations. This has important implications for the interpretation of third-harmonic generation spectra of polydiacetylenes. A resonance seen in third-harmonic generation of polydiacetylenes that has commonly been assigned as a two-photon resonance is interpreted here as a three-photon resonance.

Interest in the energy orderings of one- and two-photon states in linear-chain polyenes and oligomers of various  $\pi$ -conjugated polymers has a long history.<sup>1</sup> This ordering is a strong indicator of the relative roles of electron-electron Coulomb interactions and electron-phonon interactions in these systems,<sup>2,3</sup> a subject of continuing theoretical and experimental interest.<sup>4,5</sup> In contrast to the considerable effort that has gone into determining the energies<sup>2,3</sup> of the lowest two-photon states, there has been relatively little analysis of the *intensities* of the two-photon absorptions (TPA). Unlike linear absorption, for example, systematic studies of the chain-length dependence of TPA intensities do not exist. The observation of large nonresonant third-order optical nonlinearities in the conjugated polymers<sup>6</sup> makes it imperative that the role of TPA is precisely understood.

In this paper, we present such a discussion of TPA intensity in the correlated one-dimensional half-filled band as a function of the chain length  $N$ , where  $N$  is the number of atoms. We show that while the TPA intensity to the lowest even-parity states may initially increase with  $N$ , it soon reaches a maximum, and with further increase in chain length there is a rapid decrease of the TPA intensity. Consequently, TPA to the lowest even-parity states in the ideal infinite one-dimensional chain should be tiny for arbitrary electron-electron interactions. The dipole matrix elements that describe the TPA process also describe third-harmonic generation (THG), and our conclusion has important implications for interpretation of THG spectra of the polydiacetylenes.<sup>7-9</sup> We emphasize that our conclusion regarding TPA intensities is not necessarily valid for two-photon states that occur *above* the lowest optical state.<sup>10,11</sup> TPA intensities to such states will be discussed elsewhere.

We begin with the classification of the symmetry subspaces of even polyenes. Linear *trans*-polyenes have a center of inversion, and all eigenstates are either of even parity (hereafter  $A_g$ ) or of odd parity (hereafter  $B_u$ ) with

respect to it. As is conventional, we will assume theoretical models with electron hopping limited to nearest neighbors, in which case the  $A_g$  and the  $B_u$  states are further characterized by their electron-hole symmetries. Since dipole-allowed transitions occur only between states with opposite spatial and electron-hole symmetries, it is possible to describe the complete linear and nonlinear optical properties by retaining only those  $B_u$  states that have electron-hole symmetry opposite to that of the ground state (the  $1A_g$ ), and only those  $A_g$  states that have the same electron-hole symmetry as the  $1A_g$ . Only these optically active  $A_g$  and  $B_u$  states are considered here.

The theoretical model we choose to describe the linear polyenes is the one-dimensional extended Hubbard Hamiltonian:

$$H = U \sum_i n_{i,\uparrow} n_{i,\downarrow} + \sum_{i,j} V_{ij} (n_i - 1)(n_j - 1) - t \sum_{i,\sigma} [1 - (-1)^i \delta] [c_{i,\sigma}^\dagger c_{i+1,\sigma} + c_{i+1,\sigma}^\dagger c_{i,\sigma}]. \quad (1)$$

Here  $c_{i,\sigma}^\dagger$  creates a  $\pi$  electron of spin  $\sigma$  at site  $i$ ,  $n_{i,\sigma} = c_{i,\sigma}^\dagger c_{i,\sigma}$ ,  $n_i = \sum_\sigma c_{i,\sigma}^\dagger c_{i,\sigma}$ ,  $t > 0$  is the nearest-neighbor hopping integral,  $U$  and  $V_{ij}$  are the on-site and intersite Coulomb interactions, and  $\delta$  is the bond-alternation parameter. In all our calculations we have chosen  $t = 1$ . For most of the work presented here, we do not restrict ourselves to any specific  $U$ ,  $V_j$ , or  $\delta$ , since our motivation is to arrive at a completely general picture. We will discuss both models with short-range Coulomb interactions, as well as the chemists' Pariser-Parr-Pople (PPP) model with long-range interactions. Strictly speaking, for comparison to the polydiacetylenes, we should have three different hopping integrals. However, this makes only minor quantitative differences, and is neglected here.

For  $U = V_j = 0$ , the infinite chain one-electron spectrum has an energy gap of  $4t\delta$ . The lowest excitation is

to the  $1B_u$  across the band gap, and the lowest two-photon excited state, the  $2A_g$ , is degenerate with the  $1B_u$ . In finite polyenes, the  $2A_g$  occurs above the  $1B_u$ , as shown in Fig. 1, where we indicate the orbital occupancies of the  $1A_g$ , the  $1B_u$ , the  $2A_g$ , and the  $2B_u$ . For nonzero Coulomb interactions, no single configuration describes any of these states, and the  $2A_g$  occurs below the  $1B_u$ , which is readily understood in the limit of the strong-coupling Hubbard model ( $V_j=0$ ), where for large  $U$  the  $1A_g$  covalent (all sites are singly occupied by electrons).  $B_u$  states are necessarily ionic, and can, therefore, be reached only by charge excitation. In contrast, the lowest  $A_g$  excited states are reached by spin excitation. The same qualitative description persists even for weak Coulomb interactions. The occurrence of  $A_g$  excited states below<sup>1</sup> the  $1B_u$  is thus a strong signature of electron correlations.<sup>2,3,5</sup> Our purpose here is to estimate

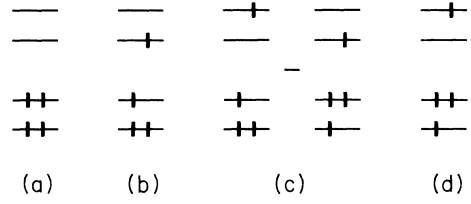


FIG. 1. The orbital occupancies of the (a)  $1A_g$ , (b)  $1B_u$ , (c)  $2A_g$ , and (d)  $2B_u$  in the limit of  $U=V_j=0$ . Only the highest two vb levels and the lowest two cb levels are shown.

TPA intensities for the class of  $A_g$  states that occur below the  $1B_u$  for infinite  $N$ .

TPA is given by the imaginary component of the third-order optical susceptibility,

$$\chi^{(3)}(-\omega; \omega, \omega, -\omega) = C \sum_{j,k,l} \frac{\langle 1A_g | \mu | jB_u \rangle \langle jB_u | \mu | kA_g \rangle \langle kA_g | \mu | lB_u \rangle \langle lB_u | \mu | 1A_g \rangle}{(\omega_{jB_u} - \omega)(\omega_{kA_g} - 2\omega)(\omega_{lB_u} - \omega)} + \dots, \quad (2)$$

where we have shown only the relevant resonant term. Here the triple sum is over all  $A_g$  and  $B_u$  states,  $C$  is a constant, and all energies are relative to the ground-state energy (i.e.,  $\hbar\omega_{1A_g}=0$ ). In analyzing TPA, the conventional assumption has been that TPA occurs at every  $\omega = \frac{1}{2}\omega_{kA_g}$ , corresponding to each zero of the denominator in Eq. (2). This is precisely why the existing analyses of TPA (and THG, see below) have been largely limited to the determination of energies alone, and little consideration has been given to intensities. We show below that because of the Pauli exclusion principle the contribution to the  $\chi^{(3)}$  is tiny in the infinite chain for certain  $A_g$  states, and thus no TPA is expected even when the corresponding energy denominators are zero.

We discuss this vanishing contribution to the  $\chi^{(3)}$  by the lowest  $A_g$  states in the noninteracting limit of  $U=0$ ,  $V_j=0$  first. In the infinite chain, interband optical transitions involving both the valence band (vb) and the conduction band (cb) are restricted between levels that are symmetrically located relative to the exact midgap, i.e., transitions are allowed only between vb levels at  $-\epsilon$  and cb levels at  $+\epsilon$ , where the zero of the energy is at the gap center. These transitions correspond to the allowed vertical transitions in the infinite periodic ring. Equation (2) then dictates the following. Two-photon transitions to any  $A_g$  state reached by single-electron excitation can occur via only *two* virtual  $B_u$  states, again placed symmetrically above and below the intraband  $A_g$  state in question. For example, in Fig. 1, the two virtual  $B_u$  states that are relevant for two-photon absorption to the  $2A_g$  are the  $1B_u$  and the  $2B_u$ . Although the  $2A_g$  is dipole coupled to other  $B_u$  states, the latter necessarily have zero dipole coupling to the  $1A_g$ , because of the restriction that allowed transitions from the ground state involves only the transitions between symmetrically placed vb and cb levels. Thus in the  $\chi^{(3)}$  expansion, correspond-

ing to each intraband  $A_g$  state, there are only four nonzero terms in the noninteracting rigid band.

We now examine the natures of these terms and again consider the  $2A_g$  for illustration. The transition dipole moments  $\langle 2A_g | \mu | 1B_u \rangle$  and  $\langle 2A_g | \mu | 2B_u \rangle$  necessarily have equal magnitudes (see Fig. 1) for all  $N$ . This is because the two transitions correspond to either the HOMO (highest occupied molecular orbital) to HOMO  $-1$  transition or the LUMO (lowest unoccupied molecular orbital) to LUMO  $+1$  transition, and the magnitudes of these are equal by electron-hole symmetry. For  $N \rightarrow \infty$ ,  $\langle 1A_g | \mu | 1B_u \rangle$  and  $\langle 1A_g | \mu | 2B_u \rangle$  are also almost equal in magnitude. Now consider the products

$$\langle 1A_g | \mu | 1B_u \rangle \langle 2A_g | \mu | 1B_u \rangle$$

and

$$\langle 1A_g | \mu | 2B_u \rangle \langle 2A_g | \mu | 2B_u \rangle.$$

These are of opposite signs because of the antisymmetric natures of the wave functions. This is easily seen by explicitly writing the singlet wave functions for the  $1B_u$ , the  $2A_g$ , and the  $2B_u$  in terms of creation operators for the band orbitals,

$$|1B_u\rangle = \frac{1}{\sqrt{2}} \sum_{\sigma} a_{N/2+1,\sigma}^{\dagger} a_{N/2,\sigma} |1A_g\rangle, \quad (3a)$$

$$|2A_g\rangle = \frac{1}{2} \sum_{\sigma} (a_{N/2+2,\sigma}^{\dagger} a_{N/2,\sigma} - a_{N/2+1,\sigma}^{\dagger} a_{N/2-1,\sigma}) |1A_g\rangle, \quad (3b)$$

$$|2B_u\rangle = \frac{1}{\sqrt{2}} \sum_{\sigma} a_{N/2+2,\sigma}^{\dagger} a_{N/2-1,\sigma} |1A_g\rangle, \quad (3c)$$

where  $a_{k,\sigma} = \sum_n \theta_{k,n} c_{n,\sigma}$  refers to a band orbital and  $|1A_g\rangle = \prod_{k < k_F} a_{k,\uparrow}^{\dagger} a_{k,\downarrow}^{\dagger} |0\rangle$ , and evaluating the matrix

elements of the dipole operator

$$\mu = \frac{1}{\sqrt{2}} \sum_{\sigma} \sum_{k_1 < k_2} m_{k_1, k_2} (a_{k_1, \sigma}^{\dagger} a_{k_2, \sigma} + a_{k_2, \sigma}^{\dagger} a_{k_1, \sigma})$$

between these states. In Eq. (4),

$$m_{k_1, k_2} = \sqrt{2} \sum_n x_n \theta_{k_1, n}^* \theta_{k_2, n},$$

and  $x_n$  gives the position of the  $n$ th atom (the electronic charge is taken to be 1). In the  $\chi^{(3)}$  expansion involving the  $2A_g$ , therefore, the signs of the two terms that contain both the  $1B_u$  and the  $2B_u$  are opposite to the two other terms that contain only the  $1B_u$  or the  $2B_u$ . The energy difference between the  $2B_u$  and the  $1B_u$  also approaches zero in the infinite chain, so that the sum of the four terms vanishes and no TPA to the  $2A_g$  would occur.

Notice that the same would be true for arbitrary band-edge  $A_g$  states reached by single-electron excitation, and TPA has vanishing intensity for all such  $A_g$  states. The overall TPA due to singly excited  $A_g$  states, however, is not zero, since  $A_g$  states reached by single-electron excitation can also be removed from the band-edge, for example, from the  $1B_u$  it is possible to reach an intraband  $A_g$  state in which the excited electron is promoted from the band edge to a level deep inside the cb. Such a high energy  $A_g$  state is shown schematically in Fig. 2. The virtual  $B_u$  state (other than the  $1B_u$ ) that is relevant now is even higher in energy, and is obtained from the  $A_g$  state in Fig. 2 by exciting an electron from a level deep inside the vb to the vb edge, as shown also schematically in Fig. 2. Even though the same sign considerations apply, the finite energy difference between the two  $B_u$  states now can lead to nonvanishing TPA away from the exact midgap.<sup>12</sup> It is clear that such processes are, however, inherently weak, and this is why calculations of THG spec-

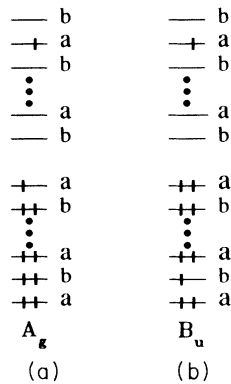


FIG. 2. (a) An  $A_g$  state ( $U=V_j=0$ ) obtained by excitation from the  $1B_u$ , upon promoting an electron from the cb edge to a level deep inside the cb (schematic); (b) the  $B_u$  state other than the  $1B_u$  that contributes to the TPA to 2(a) (schematic). This is reached from the  $2A_g$  by promoting an electron from a level deep inside the vb to the vb edge. The labels  $a$  and  $b$  refer to even- and odd-parity band levels.

tra find, at most, a kink<sup>13,14</sup> slightly above the midgap region within the rigid-band noninteracting model, as opposed to a strong two-photon resonance. To summarize, TPA to the lowest  $A_g$  states has vanishing intensity, although nonvanishing weak TPA can occur to higher energy  $A_g$  states.

We have, so far, limited our discussions to  $A_g$  states reached by single-electron excitations.  $A_g$  states that are reached by two-electron excitations are also in principle relevant in  $\chi^{(3)}$  processes. Representative examples of such two-electron excitations are shown in Fig. 3. Two-electron excitations of the type (b) in Fig. 3 make no contribution to  $\chi^{(3)}$ , because of a cancellation that has been discussed by different authors.<sup>15,16</sup> On the other hand, the contribution of configurations of type 3(a), in which all band levels are doubly occupied, do not cancel. Strong TPA should, therefore, occur at a fundamental frequency equal to the band-gap frequency. This kind of TPA is not interesting, because the linear absorption dominates in the band-gap region.

The demonstration of similar weak intensities of TPA to low-energy  $A_g$  states for *nonzero* Coulomb correlations is nontrivial, because of the intricate configuration interaction (CI) that now occurs. For example, CI studies of short correlated chains have shown that the  $2A_g$ , which occurs below the  $1B_u$ , has nearly equal contributions<sup>1(a),2</sup> from the singly excited configuration (c) in Fig. 1 and the doubly excited configuration in Fig. 3(a). Since in the noninteracting case TPA to two-electron excitations of the type in Fig. 3(a) do not cancel, it might be conjectured that Coulomb correlations should enhance TPA to  $2A_g$  and other low-lying even-parity states. We will point out the fallacy in this logic, but our demonstration of weak TPA to low-energy  $A_g$  states at  $N \rightarrow \infty$  will be based on numerical work. Since numerical work for nonzero  $U$  and  $V_j$  is limited to short finite chains, it is useful to understand the chain-length dependence of TPA to low-energy even-parity states first in the noninteracting limit, where we already understand the  $N \rightarrow \infty$  limit. We show that the direct evaluation of TPA intensity in the very short chains leads to an incorrect conclusion about the infinite chain, and indirect approaches are called for.

For what follows, we define for each  $A_g$  state with quantum number  $k$  the quantities  $\chi^+$  and  $\chi^-$ , given by

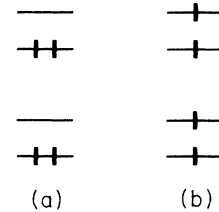


FIG. 3. Two-electron excitations in the noninteracting limit. Both (a) and (b) contribute to the  $2A_g$  for nonzero Coulomb interactions, although the contribution of (a) is much larger in short chains. These contributions are of opposite signs for all chain lengths, and the magnitudes approach each other in long chains.

$$\chi^{\pm} = \sum_j \sum_l \frac{\langle 1A_g | \mu | jB_u \rangle \langle jB_u | \mu | kA_g \rangle \langle kA_g | \mu | lB_u \rangle \langle lB_u | \mu | 1A_g \rangle}{(\omega_{jB_u} - \omega)(\omega_{lB_u} - \omega)} \quad (5)$$

Here  $\chi^+$  and  $\chi^-$  are the separate positive and negative contributions to the double sum in Eq. (5), to be calculated at frequency  $\omega = \frac{1}{2}\omega_{kA_g}$ . Clearly,  $(\chi^+ + \chi^-)$  is a measure of the TPA strength. In Fig. 4, we show the plot of  $(\chi^+ + \chi^-)$  vs  $1/N$ , calculated numerically for the  $2A_g$ , for  $\delta=0.2$  and for  $N$  up to 500. Very similar curves are obtained for several of the low-lying  $A_g$  states; only the maximum TPA and the  $N$  at which the maxima occur are different. The initial increase of  $(\chi^+ + \chi^-)$  with  $N$  is understandable within the TPA mechanism discussed above. First, for small  $N$ , allowed interband transitions are not restricted to symmetrically located occupied and unoccupied levels (i.e.,  $k$  conservation is applicable only to very large  $N$ ) and “unsymmetric”  $B_u$  states, i.e., those  $B_u$  states reached by transitions between an occupied level at  $-\epsilon$  to an unoccupied level at  $+\epsilon'$  (where  $\epsilon \neq \epsilon'$ ), make a substantial contribution to TPA. The effects of these unsymmetric  $B_u$  states do not cancel. Second, the energy difference between the  $1B_u$  and the  $2B_u$  is substantial in short noninteracting chains, and the dipole couplings  $\langle 1A_g | \mu | 1B_u \rangle$  and  $\langle 1A_g | \mu | 2B_u \rangle$  are also very different.

We now see the fundamental problem in attempting to estimate the TPA intensities at large  $N$  from direct extrapolations of the intensities at small  $N$ , an approach that works reasonably well for linear absorption. For nonzero Coulomb interactions, calculations of  $(\chi^+ + \chi^-)$  can be done only for very short chains, in a region where Fig. 4 demonstrates that TPA intensity increases with  $N$ . Direct evaluation of TPA intensities is, therefore, not suitable for estimating the intensities at  $N \rightarrow \infty$ , and an indirect approach is called for. As shown in Fig. 5, the ratio of the negative and positive contributions,  $|\chi^-/\chi^+|$ , rather than the sum, is more suitable for our purpose. Even though this ratio is small at small  $N$ , it increases

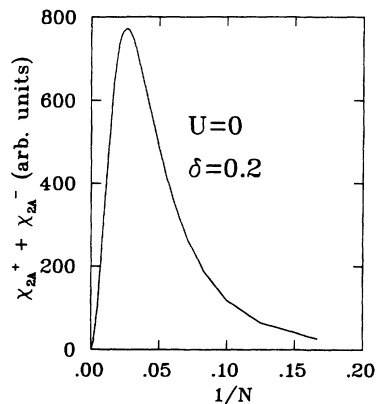


FIG. 4. The sum of the positive and the negative contributions to the TPA to  $2A_g$  in the limit of zero Coulomb interactions, as a function of the chain length  $N$ . Note that the TPA initially increases with  $N$ , but goes to zero in very long chains. A similar curve is obtained for the  $3A_g$ , with only the position of the maximum different.

continuously to reach the infinite  $N$  value.

For nonzero  $U$  and  $V_j$ , we, therefore, evaluate  $|\chi^-/\chi^+|$  for several different  $N$ . Our motivation is to demonstrate that  $|\chi^-/\chi^+|$  for low-lying  $A_g$  states (a) are *enhanced* relative to the noninteracting case, and (b) they exhibit the same monotonic behavior. In Table I we have presented the exact  $|\chi^-/\chi^+|$  for the  $2A_g$  and the  $3A_g$  for several different correlation parameters and chain lengths  $N=4, 6, 8$ . In all cases the correlation parameters are such that the  $A_g$  state in question occurs below the  $1B_u$  (for  $N=4$ , there can be only two covalent states, and, therefore, the  $3A_g$  occurs above the  $1B_u$  for arbitrarily large  $U$ ). While most of the results are for short-range Coulomb interactions, we have included the results for the PPP model with Ohno parameters<sup>17</sup> for comparison. As might be anticipated, the PPP results are comparable to those for relatively weak short-range Coulomb interactions ( $U=3$  and  $V_1=1$  in Table I). The very large values of the  $|\chi^-/\chi^+|$ , compared to the values in Fig. 1 at the same  $N$ , as well as the rapid increases with increasing  $N$ , already indicate weak TPA at infinite  $N$ . This is particularly true for  $U \geq 6$ , where  $\chi^-$  and  $\chi^+$  are nearly equal. The strong tendency of cancellation for strong Coulomb interactions is merely a signature of faster  $N \rightarrow \infty$  convergence. Note that a strong tendency to cancellation requires participation by (at least two) different  $B_u$  states, the energy difference between which should be small. Such small energy differences characterize short chains with strong Coulomb interactions, while for the same chain lengths but with weaker Coulomb interactions all energy differences are large due to the finite size effect. Since small energy differences between excited states would characterize the infinite chain even for weak Coulomb interactions, we believe that short chains with strong interactions are actually representative of much longer chains with weaker interactions.<sup>18</sup>

Unlike in the uncorrelated case, where only two  $B_u$

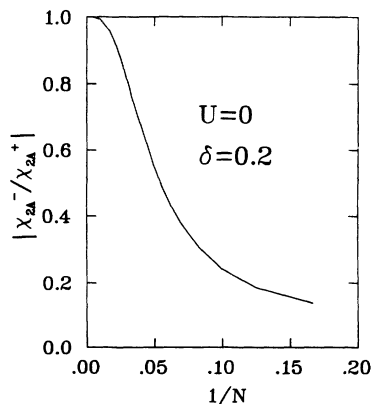


FIG. 5. The absolute value of the ratio of the negative and the positive contribution to the TPA to the  $2A_g$ , in the limit of zero Coulomb interactions, as a function of the chain length  $N$ .

states contribute to the double sums in Eq. (5) in the infinite chain, multiple  $B_u$  states contribute to these double sums (although not to the same extent) for nonzero Coulomb interactions, even in the infinite chain. Thus the calculation of  $|\chi^-/\chi^+|$  requires the complete diagonalization of the  $B_u$  subspace, as opposed to the determination of a few lowest states.<sup>3,11</sup> Currently, this can be done for at most  $N=10$  with nearly 5000  $B_u$  states. In order to determine the behavior of  $|\chi^-/\chi^+|$  at even longer  $N$ , we have, therefore, used an approximate CI technique. We start from the noninteracting limit, and

TABLE I. The exact absolute values of the ratios of the negative and the positive contributions to the TPA,  $|\chi^-/\chi^+|$ , for the  $2A_g$  and the  $3A_g$ , for  $N=4,6,8$ , and for several different Coulomb correlation parameters. For the chosen parameters the  $A_g$  states occur below the  $1B_u$ . Note the increase in the tendency to cancellation with both increasing  $N$  and increasing interactions (see text).

State	Correlation parameters	$\delta$	$N$	$ \chi^-/\chi^+ $	
$2A_g$	$U=3, V_j=0$	0.1	4	0.474	
			6	0.498	
			8	0.559	
	$U=3, V_1=1, V_j=0$ for $j>1$	0.1	4	0.495	
			6	0.486	
			8	0.514	
	$U=4, V_j=0$	0.1	4	0.659	
			6	0.706	
			8	0.794	
	$U=4, V_1=1, V_j=0$ for $j>1$	0.1	4	0.715	
			6	0.734	
			8	0.746	
	$U=6, V_1=2, V_j=0$ for $j>1$	0.1	4	0.938	
			6	0.956	
			8	0.978	
	$U=10, V_1=3, V_j=0$ for $j>1$	0.1	4	0.990	
			6	0.997	
			8	0.999	
	PPP-Ohno	0.07	4	0.452	
			6	0.514	
			8	0.532	
	$3A_g$	$U=4, V_j=0$	0.1	6	0.522
				8	0.976
			0.3	6	0.670
8				0.883	
$U=4, V_1=1, V_j=0$ for $j>1$		0.1	6	0.689	
			8	0.979	
	0.3	6	0.627		
		8	0.843		
$U=6, V_1=2, V_j=0$ for $j>1$	0.1	6	0.711		
		8	0.999		

TABLE II. The SDCI (see text)  $|\chi^-/\chi^+|$  for the  $2A_g$  for  $N=8, 16, 18$ , and 20 for several different correlation parameters. In all cases the  $2A_g$  occurs below the  $1B_u$ . The SDCI ratios are lower limits for the exact numbers (see text).

State	Correlation parameters	$\delta$	$N$	$ \chi^-/\chi^+ $	
$2A_g$	$U=3, V_j=0$	0.1	8	0.455	
			16	0.509	
			18	0.520	
			20	0.532	
			0.3	8	0.543
				16	0.682
	18	0.753			
	20	0.781			
	$U=3, V_1=1, V_j=0$ for $j>1$	0.1	8	0.437	
			16	0.460	
			18	0.473	
			20	0.488	
			0.3	8	0.628
				16	0.647
	18	0.644			
	20	0.640			
	$U=4, V_j=0$	0.1	8	0.748	
			16	0.817	
			18	0.824	
			20	0.836	
			0.3	8	0.748
				16	0.817
	18	0.824			
	20	0.836			

include CI with all singly (S) and double-excited (D) many-electron configurations (hereafter we refer to this approach as SDCI). It is known that SDCI can give the lowest  $A_g$  states below the  $1B_u$ , but the energy difference between the  $1B_u$  and the  $2A_g$  is inaccurate in long chains.<sup>19</sup> This, however, is not of concern here. We merely intend to demonstrate that the *qualitative* behavior of  $|\chi^-/\chi^+|$  is the same for the correlated and the uncorrelated cases. In Table II we show our results obtained by the SDCI approach for the  $2A_g$  for  $N=8, 16, 18$ , and 20, for a few representative parameters for which the  $2A_g$  occurs below the  $1B_u$ . We have limited ourselves to the weak Coulomb interaction regime, since Table I already indicates that for strong Coulomb interactions nearly complete cancellations occur, and since the SDCI approach becomes rather inaccurate for strong interactions. The results for the PPP-Ohno model are once again similar to those obtained for  $U=3$  and are not shown.

We now point out the following. First, the  $|\chi^-/\chi^+|$  obtained for  $N=8$  by the SDCI approach in all cases are *smaller* than the corresponding exact values (compare Tables I and II). Second, comparisons of the SDCI and exact results for  $N=4, 6$ , and 8 show that the difference between the exact and SDCI  $|\chi^-/\chi^+|$  increases with  $N$  (this is to be expected, since at the smallest  $N$ , double excitations nearly exhaust all possible excitations). Therefore, inclusion of excitations neglected within the SDCI approach actually further enhances  $|\chi^-/\chi^+|$  and the exact  $|\chi^-/\chi^+|$  for  $N=20$  in all cases must be *considerably larger* than the SDCI values in Table II. The true rate of

increase of  $|\chi^-/\chi^+|$  with  $N$  must also be larger than what is seen in Table I, from comparison of exact and SDCI results for  $N=4,6,8$ . Nevertheless, enhanced  $|\chi^-/\chi^+|$  (relative to the noninteracting model, see Fig. 4) and increase with increasing  $N$  is still observed. Finally, larger  $|\chi^-/\chi^+|$  for larger  $\delta$  is to be interpreted again as a signature of faster convergence, as occurs for strong Coulomb interactions in Table I. This is because the effect of larger  $\delta$  in short chains is also to reduce the energy gaps between  $B_u$  states. We expect similar large  $|\chi^-/\chi^+|$  for small  $\delta$  at even larger  $N$ .

The tendency to cancellation of TPA to low-energy even-parity states becomes more transparent as we probe the  $3A_g$ . In Table III, we show the  $|\chi^-/\chi^+|$  calculated for  $N=16, 18$ , and  $20$  for the  $3A_g$ . We do not compare with  $N=8$  here since the comparison may not be meaningful. The number of spin-wave excitations increases rapidly with  $N$ , and the natures of  $A_g$  excitations higher than the  $2A_g$  in systems with chain lengths differing by a factor of 2 or more are expected to be different. In short chains, we need  $U \geq 4$  to have the  $3A_g$  below the  $1B_u$ . Given that the calculated ratios are lower limits for the exact values, the very large  $|\chi^-/\chi^+|$  in this region, along with its steady increase with  $N$ , indicates near-total cancellation of the TPA at  $N \rightarrow \infty$ . It has been argued<sup>2</sup> that in long PPP chains both the  $2A_g$  and the  $3A_g$  occur below the  $1B_u$ , where a ‘‘band’’ of covalent states appear. Since there cannot be any fundamental difference between these covalent even-parity states, we believe that the cancellation seen with the  $3A_g$  is representative of the behavior of all subgap  $A_g$  states.

We now present a qualitative insight to this cancellation of the TPA. We have mentioned above that the low-energy  $A_g$  wave functions have strong contributions from doubly excited configurations for nonzero Coulomb interactions. The tendency to cancellation of the TPA may, therefore, seem counterintuitive. The tendency to cancellation still persists, because the contributions of closely related doubly excited configurations to the low-

energy  $A_g$  wave functions are themselves of opposite signs. For example, considerable discussion exists in the literature<sup>1(a),19</sup> about the contribution of configuration (a) in Fig. 3 to the interacting  $2A_g$  state. What is less recognized is that the doubly excited configuration (b) in Fig. 3 also makes a relatively large contribution [albeit smaller than 3(a) in short chains].<sup>1(a)</sup> Examination of the exact  $N=8$  results<sup>1(a)</sup> for the PPP-Ohno parameters indicates that these two contributions are of opposite signs. We find these contributions to be of opposite signs for all  $N$ ,  $U$ ,  $V_j$ , and  $\delta$  for which our exact and approximate calculations have been done. Similar phase relationships exist between all such closely related doubly excited configurations contributing to the  $2A_g$  and other low-energy two-photon states. This phase relationship can be understood by writing the Hamiltonian in Eq. (1) in molecular-orbital space ( $k$  space) and constructing the matrix elements of the electron-electron interaction term with the zeroth-order  $2A_g$  configurations in Fig. 1. It is found that the matrix elements corresponding to the two doubly excited configurations in Fig. 3 are themselves of opposite signs. In short chains, the magnitudes of these contributions are different, but in the infinite chain, these magnitudes are expected to approach each other, so that their overall contribution to the TPA should cancel. To summarize, the interacting  $2A_g$  state has contributions from both single-electron excitations of the type in Fig. 1 and two-electron excitations of the type in Fig. 3, and their overall contributions to TPA cancel via two different mechanisms. In the case of the one-electron components of the wave function, cancellation occurs because of the participation by different  $B_u$  states. In the case of the two-electron components of the wave function, the phase relationships between closely related functions is behind the tendency to cancellation. Note that this implies that the nonparticipation of configurations of the type (b) in Fig. 3 is true strictly in the limit of  $U = V_j = 0$ .

We point out that the above qualitative picture involving the phase relationships of closely related doubly excited configurations also explains diminishing transition dipole coupling between the  $2A_g$  and the lowest  $B_u$  states in finite chains with increasing Coulomb interaction. For  $N=4, 6, 8$  we have done exact calculations that find that the difference between the absolute magnitudes of the relative weights of the functions of Figs. 3(a) and 3(b) decreases monotonically with an increase in Coulomb correlations. The configuration Fig. 3(b) actually represents two different singlet functions. We choose the function reached by the direct dipole excitation from the zeroth-order  $1B_u$  and  $2B_u$  configurations, viz, the linear combination,

$$\frac{1}{2} \left[ \sum_{\sigma} a_{N/2+1,\sigma}^{\dagger} a_{N/2,\sigma} \right] \left[ \sum_{\sigma} a_{N/2+2,\sigma}^{\dagger} a_{N/2-1,\sigma} \right] |1A_g\rangle,$$

and compare its relative weight in the exact  $2A_g$  state in  $N=8$  with that of configuration Fig. 3(a), as a function of  $U$ , for the sake of illustration. These relative weights are shown in Table IV, where we have also included the exact transition dipole moments  $\langle 2A_g | \mu | 1B_u \rangle$  and

TABLE III. The SDCI  $|\chi^-/\chi^+|$  for the  $3A_g$  for  $N=16, 18$ , and  $20$  for several different correlation parameters. In all cases the  $3A_g$  occurs below the  $1B_u$ . Note the very large tendency of cancellation of TPA.

State	Correlation parameters	$\delta$	$N$	$ \chi^-/\chi^+ $	
$3A_g$	$U=4, V_j=0$	0.1	16	0.740	
			18	0.741	
			20	0.764	
		0.3	16	0.737	
			18	0.774	
			20	0.785	
	$U=4, V_1=1$	0.1	16	0.859	
			18	0.908	
			20	0.937	
		$V_j=0$ for $j>1$	0.3	16	0.933
				18	0.947
				20	0.955

TABLE IV. The exact coefficients of the configuration (a) in Fig. 3 and of the configuration (b) in Fig. 3 with singlet spin coupling between the electrons occupying the HOMO and the LUMO, and between the electrons occupying the HOMO  $-1$  and LUMO  $+1$  levels, in the  $2A_g$  state of the  $N=8$  chain for different Hubbard interactions ( $\delta=0.1$ ). The exact dipole couplings (electronic charge = 1, mean lattice constant = 1) between the  $2A_g$  and the  $1B_u$  and between the  $2A_g$  and the  $2B_u$  are also shown. Note that the individual dipole couplings decrease with  $U$ , and so do the difference between the coefficients. Similar decrease in the difference between the coefficients should occur with increasing chain length (see text).

$U$	Coefficients for 3(a)	Coefficients for 3(b)	$\langle 2A_g \mu 1B_u \rangle$	$\langle 2A_g \mu 2B_u \rangle$
2	0.4604	-0.1767	-1.2738	1.6922
3	0.4977	-0.2558	-0.5808	1.0173
4	0.4506	-0.2720	-0.3051	0.6452
5	0.3997	-0.2650	-0.1873	0.4421
6	0.3583	-0.2521	-0.1285	0.3234
20	0.1965	-0.1647	-0.0184	0.0509
100	0.1472	-0.1291	-0.0028	0.0076

$\langle 2A_g|\mu|2B_u \rangle$ . Note that the difference between the absolute magnitudes of the relative weights decreases with  $U$ , and so do the individual transition dipole moments. Similar results are obtained for other pairs of closely related double excitations. Note that the above qualitative picture also is an indirect confirmation of our idea that strongly interacting short chains give qualitative insights to the behavior of weakly interacting long chains.

From the behavior of  $|\chi^-/\chi^+|$  in Tables I–III we conclude that TPA to  $A_g$  states below the  $1B_u$  is tiny in the

infinite chain limit. This weak role of low-energy two-photon states should also be true for other  $\chi^{(3)}$  processes, for which the relevant dipole matrix elements are the same and only the energy denominators are different. Most importantly, we show that our conclusion has strong implications for the interpretation of the THG spectra in the polydiacetylenes.<sup>7–9</sup>

For what follows, we explicitly write the formal expression for the relevant resonant term in the THG susceptibility,

$$\chi^{(3)}(-3\omega; \omega, \omega, \omega) = C \sum_{jkl} \frac{\langle 1A_g|\mu|jB_u \rangle \langle jB_u|\mu|kA_g \rangle \langle kA_g|\mu|lB_u \rangle \langle lB_u|\mu|1A_g \rangle}{(\omega_{jB_u} - 3\omega)(\omega_{kA_g} - 2\omega)(\omega_{lB_u} - \omega)} + \dots \quad (6)$$

Three-photon resonances to  $B_u$  states and two-photon resonances to  $A_g$  states are expected now. In ordered long chain polydiacetylenes, the lowest optical exciton occurs at about 1.9–2.0 eV, and it is believed that the conduction-band threshold<sup>20</sup> is at 2.4–2.5 eV, a region where there is practically no linear absorption. In THG experiments carried out so far,<sup>7–9</sup> the fundamental frequency ranges from 0.5–0.6 eV in the low-frequency region to 1.2–1.5 eV in the high-frequency region. Two distinct resonances are seen in the ordered systems, a strong one at 0.65–0.7 eV, and a relatively weaker one at about 0.8–0.9 eV. The former is easily assigned as a three-photon resonance to the  $1B_u$  exciton. Because of the absence of linear absorption at three times the second resonant frequency, the higher-frequency resonance has commonly been assigned<sup>7,11</sup> to a two-photon resonance to the  $2A_g$ , which is known to occur below<sup>1(b)</sup> the  $1B_u$  absorption (note, however, that the exact location of the  $2A_g$  in the polymer is not known from theoretical considerations alone, and there exists no other independent experimental verification of the energy assignment). While from energy considerations such an assignment seems plausible, our discussion of the role of the  $2A_g$  in TPA processes in long chains suggests that this is a highly unlikely scenario from intensity considerations. The intensity of the resonance at 0.8 eV is rather strong, and

from eye estimates can be as large as  $\frac{1}{4}$  of the intensity of the lower-frequency resonance.<sup>7</sup> We present an analysis of the intensity of the two-photon resonance to the  $2A_g$  in THG that indicates that the origin of the resonance at the higher frequency in the polydiacetylenes is different. Before we present such an analysis we first briefly discuss an alternate interpretation of the second THG resonance that has been given recently by two different groups.<sup>18,21–23</sup>

Within the second model,<sup>18,21–23</sup> the resonance near 0.8 eV is not a two-photon resonance at all, but a three-photon resonance to the conduction-band threshold at 2.4 eV, which is a  $B_u$  state. In the work by Guo and co-workers,<sup>18,21</sup> this  $B_u$  state is referred to as the  $nB_u$ , where  $n$  is an arbitrary quantum number whose value depends on both the chain length as well as the actual Coulomb correlation parameters. For nonzero Coulomb interactions,  $n > 2$ , and all states of either parity below the  $nB_u$  are excitonic. Direct dipole coupling from the  $1A_g$  to the  $nB_u$  is very weak for nonzero intersite Coulomb interactions, and, therefore, the conduction-band threshold is not visible in linear absorption. Nevertheless, the  $nB_u$  participates strongly in  $\chi^{(3)}$  processes because of the occurrence of a two-photon exciton that occurs above the  $1B_u$  and below the  $nB_u$ , and which is very strongly dipole coupled to both these  $B_u$  states. Our previous work<sup>10,18</sup>

refers to this two-photon state as the  $m A_g$ , where again  $m$  is an arbitrary quantum number that depends on the actual chain length and the Coulomb parameters. Independent of the chain length and the parameters, however, the dipole coupling between the  $1B_u$  and the  $m A_g$  is enormously large<sup>10</sup> compared to the dipole coupling between the  $1B_u$  and all other  $A_g$  states. The  $m A_g$  has a similar giant dipole coupling with the  $nB_u$  above it. Detailed wave-function analyses<sup>18,21</sup> as well as comparison of experimental and theoretical electro-absorption spectra<sup>18,21</sup> have shown that the  $nB_u$  is indeed the conduction-band threshold. In short chains the absolute energies of the  $m A_g$  and the  $nB_u$  are rather high because of the inherent discrete nature of finite chain spectra, but the demonstration of the delocalized band threshold character of the  $nB_u$  proves that in the infinite chain the  $nB_u$  occurs at 2.4 eV, and, therefore, the energy of the  $m A_g$  is even lower. Three out of four dipole couplings in the nonlinear optical channel  $1A_g \rightarrow 1B_u \rightarrow m A_g \rightarrow nB_u \rightarrow 1A_g$  are exceptionally large, indicating strong participation by the  $nB_u$  in  $\chi^{(3)}$  processes, and a three-photon resonance at  $\frac{1}{3}\hbar\omega_{nB_u} = 0.8$  eV.

The interpretation of optical nonlinearity in the polydiacetylenes given independently by Abe *et al.*,<sup>22,23</sup> is very

$$I_{3\omega}(1B_u) = \sum_k \sum_l \frac{\langle 1A_g | \mu | 1B_u \rangle \langle 1B_u | \mu | k A_g \rangle \langle k A_g | \mu | l B_u \rangle \langle l B_u | \mu | 1A_g \rangle}{(\omega_{kA_g} - 2\omega)(\omega_{lB_u} - \omega)}, \quad (7a)$$

$$I_{3\omega}(nB_u) = \sum_k \sum_l \frac{\langle 1A_g | \mu | nB_u \rangle \langle nB_u | \mu | k A_g \rangle \langle k A_g | \mu | l B_u \rangle \langle l B_u | \mu | 1A_g \rangle}{(\omega_{kA_g} - 2\omega)(\omega_{lB_u} - \omega)}, \quad (7b)$$

while for the two-photon resonance to the  $2A_g$  we define

$$I_{2\omega}(2A_g) = \sum_j \sum_l \frac{\langle 1A_g | \mu | j B_u \rangle \langle j B_u | \mu | 2A_g \rangle \langle 2A_g | \mu | l B_u \rangle \langle l B_u | \mu | 1A_g \rangle}{(\omega_{jB_u} - 3\omega)(\omega_{lB_u} - \omega)}. \quad (7c)$$

Here  $I_{3\omega}(1B_u)$ ,  $I_{3\omega}(nB_u)$ , and  $I_{2\omega}(2A_g)$  are direct measures of the intensities of the three-photon resonance to the  $1B_u$ , the three-photon resonance to the  $nB_u$ , and the two-photon resonance to the  $2A_g$ . They are to be calculated at  $\omega = \frac{1}{3}\omega_{1B_u}$ ,  $\omega = \frac{1}{3}\omega_{nB_u}$ , and  $\omega = \frac{1}{2}\omega_{2A_g}$ , respectively. Note that  $I_{2\omega}(2A_g)$  again has contributions of opposite signs, since the origin of the different signs is in the numerator and not the denominator in Eq. (7c). All calculations involved exact dipole matrix elements obtained for  $N=8$  with PPP-Ohno<sup>17</sup> and PPP-Mataga-Nishimoto<sup>24</sup> (MN) parameters (results for other Coulomb parameters are not shown since they are very similar). The calculation of  $I_{2\omega}(2A_g)$  involved also the exact finite chain energies, since our result for TPA intensities establishes that the  $I_{2\omega}(2A_g)$  obtained for finite chains is an absolute upper limit for the  $I_{2\omega}(2A_g)$  in the infinite chain. Calculations of  $I_{3\omega}(1B_u)$  and  $I_{3\omega}(nB_u)$ , however, cannot be done with exact finite chain energies, because of two reasons. First, the energies of the  $m A_g$  and the

similar. These authors also find a two-photon exciton in between the  $1B_u$  exciton and the conduction-band threshold, emphasize the strong role of the particular  $\chi^{(3)}$  channel discussed above, and claim that the observed 0.8-eV resonance in the polydiacetylenes is a three-photon resonance to the band threshold state. However, the computation by Abe *et al.* is done within a single-CI scheme that includes only single-electron excitations from the noninteracting limit, and, therefore, does not find  $A_g$  states below the  $1B_u$ . The very possibility of a two-photon resonance at 0.8 eV is, therefore, missing in this work. The similarity between our interpretation of THG spectra in the polydiacetylenes, based on short-chain calculations that do find the  $2A_g$  below the  $1B_u$ , and that by Abe *et al.*<sup>22,23</sup> which are for long chains but which do not find  $A_g$  states below the  $1B_u$ , is thus surprising. This similarity can be understood only from analysis of the intensities of the various THG resonances, as is done below.

In analogy with our calculations of TPA intensities, we define the quantities that are related to the intensities of the various THG resonances as double sums. For the three-photon resonance to the  $1B_u$  and the  $nB_u$ , we consider the double sums,

$nB_u$  are too high in short chains.<sup>10(b)</sup> Second, finite PPP chains give double resonances,<sup>25</sup> two-photon resonance to the  $m A_g$  and three-photon resonance to the  $nB_u$  occurring at nearly the same frequency, due to the highly discrete energy spectrum (actually such double resonances would occur in all weakly interacting short chains, including the noninteracting model<sup>26</sup>). Thus the exact energy spectrum would predict a stronger<sup>25</sup> three-photon resonance to the  $nB_u$  than to the  $1B_u$ , clearly not an infinite chain result. Fortunately, both these problems can be resolved from consideration of the following. The double sums in Eqs. 7(a) and 7(b) are given almost entirely by a few dominant terms because of the large dipole couplings between the  $1B_u$  and the  $m A_g$  and between the  $nB_u$  and the  $m A_g$  on the one hand, and the very weak couplings between all other relevant states on the other.<sup>10,18,21</sup> Very reliable estimates of  $I_{3\omega}(1B_u)$  and  $I_{3\omega}(nB_u)$  are, therefore, obtained from the following expressions,



$$I_{3\omega}(1B_u) \simeq \frac{\langle 1A_g|\mu|1B_u\rangle^4}{(\omega_{1B_u}-\omega)(-2\omega)} + \frac{\langle 1A_g|\mu|1B_u\rangle^2\langle 1B_u|\mu|mA_g\rangle^2}{(\omega_{1B_u}-\omega)(\omega_{mA_g}-2\omega)} + \frac{\langle 1A_g|\mu|1B_u\rangle\langle 1B_u|\mu|mA_g\rangle\langle mA_g|\mu|nB_u\rangle\langle nB_u|\mu|1A_g\rangle}{(\omega_{nB_u}-\omega)(\omega_{mA_g}-2\omega)}, \quad (8a)$$

$$I_{3\omega}(nB_u) \simeq \frac{\langle 1A_g|\mu|1B_u\rangle\langle 1B_u|\mu|mA_g\rangle\langle mA_g|\mu|nB_u\rangle\langle nB_u|\mu|1A_g\rangle}{(\omega_{1B_u}-\omega)(\omega_{mA_g}-2\omega)}. \quad (8b)$$

In Eq. (8a) all dominant terms have been retained, but terms in which two or more of the dipole couplings are weak have been discarded. The estimates of the *relative* magnitudes of  $I_{3\omega}(1B_u)$  and  $I_{3\omega}(nB_u)$  in the infinite chain can now be obtained by substituting the exact finite chain transition dipole moments with the *infinite* chain energies of the  $1B_u$  and the  $nB_u$  in Eqs. (8a) and (8b). We substitute the experimental exciton energy and the conduction-band threshold energy for the energies of the  $1B_u$  and the  $nB_u$  in our calculations. Since we are interested in relative quantities, the only assumption in the above procedure is that all transition dipole moments in Eqs. (8a) and (8b) increase with  $N$  in a similar fashion. This is certainly a reasonable assumption. Note that since all transition dipole couplings in Eq. (8b) increase with  $N$ , and since the tendency to cancellation of the two-photon resonance to  $2A_g$  also increases with  $N$ , our calculations will necessarily give an upper limit for  $I_{2\omega}(2A_g)/I_{3\omega}(nB_u)$ . The energy of the  $mA_g$  is the only uncertain quantity in Eqs. (8a) and (8b). We have placed the  $mA_g$  at 2.2 eV somewhat arbitrarily. We have verified that the relative intensities are independent of its actual location, as long as it is placed in between the  $1B_u$  and the  $nB_u$ , in agreement with finite chain results.<sup>10,18,21</sup>

The numerical results for the relative intensities of the two three-photon resonances and the two-photon resonance to the  $2A_g$  are shown in Table V for the PPP-Ohno and the PPP-MN parameters (the  $mA_g$  and the  $nB_u$  are found by the procedures discussed before<sup>10,21</sup>). As discussed above, within our approximation, the relative strength of the  $2A_g$  two-photon resonance, compared to the three-photon resonance to the  $nB_u$ , is an absolute upper limit. Nevertheless, it is seen that the intensity of the  $2A_g$  two-photon resonance is tiny. Comparison to the experimental THG spectra in the polydiacetylenes<sup>7-9</sup> clearly indicates that the 0.8-eV resonance is a second three-photon resonance. The calculated intensity of the second three-photon resonance, relative to the calculated intensity of the three-photon resonance to the  $1B_u$  exciton, is close to what are experimentally observed.<sup>7,8</sup>

The conclusion that the 0.8-eV resonance in THG is a three-photon resonance to the  $nB_u$  is also supported by

comparison of electro-absorption and THG spectra. Hasegawa *et al.* have performed both electro-absorption and THG on the same blue form of a polydiacetylene film<sup>8</sup> which shows a narrow excitonic linear absorption at 2 eV. The electro-absorption spectrum indicates that the energy of the conduction-band threshold is 2.4 eV. The second resonance in THG is at one-third this energy, and the present work indicates that this is not a coincidence. That the  $2A_g$  contributes very weakly to the third-order optical nonlinearity is seen from the result of the electro-absorption measurement at energies below the region where the Stark shift of the  $1B_u$  exciton is observed. For this particular material the authors' electro-absorption measurements extend down to 1.35 eV, but there is a complete absence of any field-induced signal<sup>18(b)</sup> from the  $2A_g$ , even though it is known<sup>1(b)</sup> that the  $2A_g$  occurs below the  $1B_u$ . This is in agreement with the present conclusion [since electro-absorption is also a  $\chi^{(3)}$  process with the same numerator as in Eqs. (2) and (4), and the cancellation depends only on terms with opposite signs in the numerator], as well as with our previous nonperturbative calculation of the electro-absorption<sup>21</sup> in the energy region below the  $1B_u$ .

Since the contributions of the low-energy  $A_g$  states to optical nonlinearity in long chains is tiny, optical nonlinearity is dominated by the four essential states, the  $1A_g$ , the  $1B_u$ , the  $mA_g$ , and the  $nB_u$ . In addition to the two three-photon resonances, a weak two-photon resonance at 1.0–1.2 eV to the  $mA_g$  is then expected. We have previously shown from finite chain calculations with very large Coulomb interactions ( $U=10$ ,  $V_1=3.5$ ) that such a three-peak THG spectrum is obtained even when all exact excited-state energies and dipole moments are retained in the calculation<sup>21</sup> (no double resonance occurs here because “band” formation can occur because of the very large Coulomb interaction). Very few of the experimental THG spectra cover the entire frequency range of interest and we are aware of only two experiments that do so. Close examination of the THG spectrum obtained for a polydiacetylene film by Kajzar and Messier<sup>7</sup> indicates not only the two resonances discussed by the authors (at 1.907 and 1.35  $\mu\text{m}$ ), but also a weak (but dis-

TABLE V. The relative intensities of the  $2A_g$  two-photon resonance, the  $1B_u$  three-photon resonance, and the  $nB_u$  three-photon resonance in THG, within the PPP-Ohno and the PPP-MN models (see text). The relative intensity of the  $2A_g$  two-photon resonance is an absolute upper limit (see text).

Parameter	$I_{2\omega}(2A_g)$	$I_{3\omega}(1B_u)$	$I_{3\omega}(nB_u)$	$I_{3\omega}(nB_u)/I_{3\omega}(1B_u)$
PPP-Ohno	0.2878	8.5349	1.1869	0.1391
PPP-MN	0.2838	7.3589	2.4775	0.3367

inct) shoulder at 1.1  $\mu\text{m}$ . We believe that the experimental THG spectrum here does indicate three resonances, as discussed above. Note that the frequency range covered here very clearly precludes the 1.35  $\mu\text{m}$  resonance from being a  $2A_g$  two-photon resonance, since even in finite chains the two-photon resonance to the  $2A_g$  is considerably *weaker* than the two-photon resonance to the  $mA_g$ , which should appear at higher frequency.<sup>10,11</sup> No such signature of a stronger two-photon resonance at shorter wavelengths is seen in the experiment of Kajzar and Messier, although the experimental data points go down to about 0.8  $\mu\text{m}$  in wavelength (up to about 1.55 eV in energy), and should have, therefore, found all two-photon states up to 3.1 eV. The only choice is to assign the 1.35  $\mu\text{m}$  resonance to the three-photon resonance to the  $nB_u$ . The same conclusion is reached from examination of the very recent THG study of Hasegawa *et al.*, who have extended their study of the polydiacetylene blue film investigated earlier<sup>8</sup> all the way to 1.7 eV.<sup>27</sup> In addition to the strong resonances at 0.65 and 0.8 eV, a weak structure is seen at about 1.2 eV, but no other strong resonance is seen at higher energies.

To summarize, we have presented detailed calculations of intensities of TPA to  $A_g$  states occurring below the  $1B_u$  which indicate that in the ideal infinite chain such states make negligible contribution to third-order optical nonlinearity. Analysis of intensities of three-photon and two-photon resonances in THG indicate that the 0.8-eV resonance in the polydiacetylenes is a three-photon resonance due to the conduction-band threshold and is not a two-photon resonance. The success of the single-CI model of Abe *et al.*<sup>22,23</sup> can be understood within this context. The single-CI approach misses the  $A_g$  states below the optical exciton, but is able to capture the behavior of higher-energy two-photon excitons and the conduction-band threshold that dominate nonlinear optical behavior in long chains. There does exist, however, one additional difference between the single-CI model and our work. We expect biexcitons above the  $mA_g$  in our model with relatively large binding energies. These will be discussed elsewhere.

We have restricted ourselves to  $A_g$  states below the  $1B_u$  in the present work, but very similar cancellations will also occur for many of the (but not all)  $A_g$  states that occur above the  $1B_u$  but below the conduction band. This has important implications for two-photon absorption experiments in aromatic conjugated polymers in which the  $2A_g$  occurs above the  $1B_u$ . Sharp TPA is often found,<sup>28,29</sup> and sometimes<sup>28</sup> is assigned to the  $2A_g$ . We believe that the actual quantum number of the dominant  $A_g$  state is uncertain, and may not necessarily be two (in our theoretical work the quantum number  $m$  of the dominant two-photon state ranges from two to a chain length and correlation dependent saturation number<sup>10</sup>). It is conceivable that the observed two-photon states in these systems is a still higher  $A_g$  state, and TPA to all lower  $A_g$  states (which are however above the  $1B_u$  in this case) are weak due to cancellations similar to that described here. The situation could be thus very similar to that in *trans*-polyacetylene, for which it has now become clear that the two-photon resonance seen in THG is not the  $2A_g$ , even though this was assumed to be so in the original paper.<sup>30</sup> Finally, recent work by various authors<sup>31,32</sup> have emphasized the saturation behavior of the nonresonant third-order optical nonlinearity in linear polyenes as the chain length is increased. Our work here presents a detailed mechanism of this saturation. With increasing chain length, the contributions of the bulk of the  $A_g$  states to the nonlinearity vanish because of the cancellations described here, and, therefore, the nonlinearity is derived from a few dominant terms involving the essential states. Once convergence in the energies of these essential states and the transition dipole couplings between them have been reached at a certain  $N$ , saturation in the third-order nonlinearity is to be expected.

The authors acknowledge support from NSF (Grant No. ECS-89-11960) and from the AFOSR (Grant No. F49620-93-1-0199). We are grateful to Professor T. Koda (University of Tokyo) for kindly sending his unpublished THG results.

<sup>1</sup>(a) B. S. Hudson, B. E. Kohler, and K. Schulten, in *Excited States 6*, edited by E. C. Lim (Academic, New York, 1982); (b) B. E. Kohler and D. E. Schilke, *J. Chem. Phys.* **86**, 5214 (1987).

<sup>2</sup>P. Tavan and K. Schulten, *Phys. Rev. B* **36**, 4337 (1987), and references therein.

<sup>3</sup>Z. G. Soos and S. Ramasesha, *Phys. Rev. B* **29**, 5410 (1984), and references therein.

<sup>4</sup>A. J. Heeger, S. Kivelson, J. R. Schrieffer, and W. P. Su, *Rev. Mod. Phys.* **60**, 781 (1988).

<sup>5</sup>D. Baeriswyl, D. K. Campbell, and S. Mazumdar, in *Conjugated Conducting Polymers*, edited by H. Kiess (Springer-Verlag, Berlin, 1992), pp. 7–133.

<sup>6</sup>*Nonlinear Optical Properties of Organic Molecules and Crystals*, edited by D. S. Chemla and J. Zyss (Academic, New York, 1987).

<sup>7</sup>F. Kajzar and J. Messier, *Thin Solid Films* **132**, 11 (1985).

<sup>8</sup>(a) T. Hasegawa, K. Ishikawa, T. Kanetake, T. Koda, K. Takeda, H. Kobayashi, and K. Kubodera, *Chem. Phys. Lett.* **171**,

239 (1990); (b) T. Hasegawa, K. Ishikawa, T. Koda, K. Takeda, H. Kobayashi, and K. Kubodera, *Synth. Metals* **41-43**, 3151 (1991).

<sup>9</sup>W. E. Torruellas, K. B. Rochford, R. Zanoni, S. Aramaki, and G. I. Stegeman, *Opt. Commun.* **82**, 94 (1991).

<sup>10</sup>(a) S. N. Dixit, D. Guo, and S. Mazumdar, *Phys. Rev. B* **43**, 6781 (1991); (b) S. Mazumdar, D. Guo, and S. N. Dixit, *J. Chem. Phys.* **96**, 6862 (1992).

<sup>11</sup>P. C. M. McWilliams, G. W. Hayden, and Z. G. Soos, *Phys. Rev. B* **43**, 9777 (1991).

<sup>12</sup>G. P. Agrawal, C. Cojan, and C. Flytzanis, *Phys. Rev. B* **17**, 776 (1978).

<sup>13</sup>J. Yu, B. Friedman, P. R. Baldwin, and W.-P. Su, *Phys. Rev. B* **39**, 12 814 (1989).

<sup>14</sup>Chang-qin Wu and Xin Sun, *Phys. Rev. B* **41**, 12 845 (1990).

<sup>15</sup>Z. G. Soos, G. Hayden, and P. C. McWilliams, in *Conjugated Polymeric Materials: Opportunities in Electronics, Optoelectronics and Molecular Electronics* (Kluwer, Dordrecht, 1990), pp. 495–508.

- <sup>16</sup>Z. Shuai and J. L. Bredas, *Phys. Rev. B* **44**, 5962 (1991).
- <sup>17</sup>K. Ohno, *Theor. Chim. Acta* **2**, 219 (1964).
- <sup>18</sup>Y. Kawabe, F. Jarka, N. Peyghambarian, D. Guo, S. Mazumdar, S. N. Dixit, and F. Kajzar, *Phys. Rev. B* **44**, 6530 (1991).
- <sup>19</sup>I. Ohmine, M. Karplus, and K. Schulten, *J. Chem. Phys.* **68**, 2298 (1978).
- <sup>20</sup>K. C. Yee and R. R. Chance, *J. Polym. Sci. Polym. Phys. Ed.* **16**, 431 (1978).
- <sup>21</sup>D. Guo, S. Mazumdar, S. N. Dixit, F. Kajzar, F. Jarka, Y. Kawabe, and N. Peyghambarian, *Phys. Rev. B* **48**, 1433 (1993); see also D. Guo, S. Mazumdar, and S. N. Dixit, *Proceedings of the International Conference on Synthetic Metals, ICSM 92* [*Synth. Metals* **55-57**, 3881 (1993)].
- <sup>22</sup>S. Abe, M. Schreiber, W. P. Su, and J. Yu, *Phys. Rev. B* **45**, 9432 (1992); see also, *J. Lumin.* **53**, 519 (1992).
- <sup>23</sup>S. Abe, in *Relaxation in Polymers*, edited by T. Kobayashi (World Scientific, Singapore, in press).
- <sup>24</sup>N. Mataga and K. Nishimoto, *Z. Phys. Chem. Neue Folge* **13**, 140 (1957).
- <sup>25</sup>D. Guo and S. Mazumdar, *J. Chem. Phys.* **97**, 2170 (1992).
- <sup>26</sup>Chang-qin Wu and X. Sun, *Phys. Rev. B* **42**, 9736 (1990).
- <sup>27</sup>T. Hasegawa, H. Kishida, Y. Iwasa, K. Ishikawa, T. Koda, K. Takeda, H. Kobayashi, K. Kubodera, T. Wada, H. Tashiro, and S. Abe (unpublished). A preliminary discussion may be found in, T. Hasegawa, K. Ishikawa, T. Koda, H. Takeda, H. Kobayashi, and K. Kubodera, *Synth. Metals* **49-50**, 123 (1992).
- <sup>28</sup>N. Periasamy, R. Danieli, G. Ruani, R. Zamboni, and C. Tali-ani, *Phys. Rev. Lett.* **68**, 919 (1992).
- <sup>29</sup>N. Pfeffer, P. Raimond, F. Charra, and J. M. Nunzi, *Chem. Phys. Lett.* **201**, 357 (1993).
- <sup>30</sup>W. S. Fann, S. Benson, J. M. J. Madey, S. Etemad, G. L. Baker, and F. Kajzar, *Phys. Rev. Lett.* **62**, 1492 (1989).
- <sup>31</sup>S. Mukamel and H. Wang, *Phys. Rev. Lett.* **69**, 65 (1992).
- <sup>32</sup>D. Yaron and R. Silbey, *Phys. Rev. B* **45**, 11 655 (1992).